THE JOURNAL OF BIOLOGICAL CHEMISTRY VOL. 288, NO. 15, pp. 10819–10829, April 12, 2013

Hypoxia-inducible Factor 1 (HIF-1) Promotes Extracellular Matrix Remodeling under Hypoxic Conditions by Inducing *P4HA1*, *P4HA2*, and *PLOD2* Expression in Fibroblasts*[S]

Received for publication, December 6, 2012, and in revised form, January 17, 2013 Published, JBC Papers in Press, February 19, 2013, DOI 10.1074/jbc.M112.442939

Daniele M. Gilkes[‡§¶1], **Saumendra Bajpai**[¶‖], **Pallavi Chaturvedi**[‡§], **Denis Wirtz**[¶‖], **and Gregg L. Semenza**[‡§¶**2]

From the [‡]*Vascular Program, Institute for Cell Engineering,* [§]*McKusick-Nathans, Institute of Genetic Medicine, and* **Departments *of Pediatrics, Oncology, Medicine, Radiation Oncology, and Biological Chemistry, the Johns Hopkins University School of Medicine, Baltimore, Maryland 21205, and the* [¶]*Johns Hopkins Physical Sciences, Oncology Center, and* [‖]*Department of Chemical and Biomolecular Engineering, The Johns Hopkins University, Baltimore, Maryland 21218*

Background: In hypoxic cells, HIF-1 transactivates genes with roles in developmental, physiological, and disease processes.
Results: HIF-1 activity in hypoxic fibroblasts promotes extracellular matrix (ECM) remodeling by inducing expression of the collagen hydroxylases P4HA1, P4HA2, and PLOD2.
Conclusion: HIF-1 stimulates ECM fiber alignment, which influences cell morphology, adhesion, and directional migration.
Significance: Hypoxia induces changes in ECM that have non-cell-autonomous effects on cell behavior.

Extracellular matrix (ECM) composition, organization, and compliance provide both architectural and chemical cues that modulate tissue structure and function. ECM produced by stromal fibroblasts plays a key role in breast cancer invasion and metastasis, which are also stimulated by intratumoral hypoxia. Here, we demonstrate that hypoxia-inducible factor 1 (HIF-1) is a critical regulator of ECM remodeling by fibroblasts under hypoxic conditions. HIF-1 activates expression of genes encoding collagen prolyl (P4HA1 and P4HA2) and lysyl (PLOD2) hydroxylases. P4HA1 and P4HA2 are required for collagen deposition, whereas PLOD2 is required for ECM stiffening and collagen fiber alignment. Together P4HA1, P4HA2, and PLOD2 mediate remodeling of ECM composition, alignment, and mechanical properties in response to hypoxia. HIF-1-dependent ECM remodeling by hypoxic fibroblasts induces changes in breast cancer cell morphology, adhesion, and motility that promote invasion and metastasis.

The extracellular matrix (ECM)[3] provides a physical framework for cells and initiates biochemical and biomechanical interactions that are required for key cellular events such as adhesion, migration, proliferation, differentiation, and survival. The ECM directs cellular organization by interacting with cell surface receptors to promote the activation of signal transduction pathways that lead to a variety of physiological responses. The ECM is important for diverse physiological and pathological processes from embryogenesis to cancer cell invasion and metastasis (1, 2). A wide range of diseases result from genetic abnormalities involving ECM proteins (3).

Collagens, which are the most abundant proteins in the human body, provide a scaffold for ECM assembly. Collagens comprise a large family of structurally related proteins, each containing a unique triple helical structure formed by repeating *GXY* sequences (where G is glycine, *X* is often proline or lysine, and *Y* is often hydroxyproline). Collagen biogenesis is a complex process involving extensive post-translational modifications, particularly the hydroxylation of prolyl and lysyl residues (4).

Collagen prolyl 4-hydroxylases (P4Hs) catalyze the formation of 4-hydroxyproline from proline residues. P4Hs are essential for collagen biogenesis because 4-hydroxyproline residues are necessary for the proper folding of collagen polypeptide chains into stable triple helical molecules (4, 5). Three isoforms of the P4HA subunit have been identified (P4HA1, P4HA2, and P4HA3) that form A_2B_2 tetramers with P4HB resulting in P4H1, P4H2, and P4H3 holoenzymes, respectively (6, 7).

The pattern and extent of collagen lysyl hydroxylation influence the stability of intermolecular collagen cross-links that provide the tensile strength and mechanical stability of collagen fibrils and serve as attachment sites for carbohydrates. Three genes (*PLOD1*, *PLOD2*, and *PLOD3*) encoding unique isoforms of procollagen-lysine, 2-oxoglutarate 5-dioxygenase have been characterized (8). PLOD1 and PLOD2 hydroxylate lysine residues in the triple helical and telopeptide domains, respectively, whereas the substrate specificity of PLOD3 is unknown (9, 10). Mutations in *PLOD1* or *PLOD2* cause Ehlers-Danlos syndrome type VIA (11) and Bruck syndrome (12), respectively. Increased collagen lysyl hydroxylation by PLOD2 promotes fibrosis (13).

* This work was supported in part by National Institutes of Health Grant U54-CA143868 through the NCI. This work was also supported by American Cancer Society Grant 122437-RP-12-090-01-COUN.
[S] This article contains supplemental Figs. S1–S4 and Movies S1–S6.
[1] Recipient of a Susan G. Komen Breast Cancer Foundation postdoctoral fellowship award.
[2] C. Michael Armstrong Professor at the Johns Hopkins University School of Medicine and an American Cancer Society Research Professor. To whom correspondence should be addressed: Depts. of Pediatrics, Medicine, Oncology, Radiation Oncology, Biological Chemistry, and Genetic Medicine, Johns Hopkins University School of Medicine, 733 North Broadway, Suite 671, Baltimore, MD 21205. Fax: 443-287-5618; E-mail: gsemenza@jhmi.edu.
[3] The abbreviations used are: ECM, extracellular matrix; ANOVA, analysis of variance; EV, empty vector; HIF, hypoxia-inducible factor; MSC, mesenchymal stem cell; P4H, prolyl 4-hydroxylase; pC, C-terminal propeptide; pN, N-terminal propeptide; PLOD, procollagen-lysine, 2-oxoglutarate 5-dioxygenase.

Hypoxia has been shown to induce the expression of mRNAs encoding for P4HA1, P4HA2, PLOD1, and PLOD2 in various cell types (14, 15). Hypoxia has also been proposed as an important microenvironmental factor that stimulates tissue fibrosis (16–18). In cancer, intratumoral hypoxia is associated with increased risk of invasion, metastasis, treatment failure, and patient mortality (19). Hypoxia-inducible factor 1 (HIF-1) and HIF-2 are key mediators of cellular adaptation to low oxygen conditions. HIF-1 is a heterodimeric transcription factor consisting of a constitutively expressed HIF-1β subunit and an O_2-regulated HIF-1α subunit (20). Under conditions of reduced O_2 availability, HIF-1α protein is stabilized, dimerizes with HIF-1β, and activates transcription of target genes that play key roles in development, physiology, and diseases such as cancer (21, 22).

Both increased HIF-1α protein levels (23–27) and the pattern and extent of collagen deposition and alignment (28) in tumor biopsies are independently predictive of cancer patient mortality. *In vivo* imaging has shown that tumor cells preferentially invade along straightened, aligned collagen fibers produced by stromal cells to promote intravasation (29–31). However, the contribution of HIF-1 activity in hypoxic human stromal cells to collagen deposition and fiber alignment has not been reported.

The role of HIF-1 in P4HA1 and P4HA2 mRNA expression and enzyme activity in mouse chondrocytes was recently reported (32). In this report, we show that HIF-1-regulated collagen prolyl and lysyl hydroxylase expression affects the composition and mechanical properties of human fibroblast-derived ECM. We demonstrate that HIF-1α-dependent expression of collagen prolyl and lysyl hydroxylases is required for proper collagen fiber formation in response to hypoxia. We also show for the first time the role of P4HA1, P4HA2, and PLOD2 expression in collagen deposition by human cells. We demonstrate the contribution of HIF-1-regulated ECM remodeling to matrix stiffness and show that HIF-1-regulated ECM production and alignment dictate cell-matrix interactions that promote cancer cell spreading, adhesion, and directional migration using a novel technique to image three-dimensional matrix-regulated cell motility.

EXPERIMENTAL PROCEDURES

Cell Culture—Human newborn foreskin fibroblasts (ATCC), MDA-MB-231 cells (NCI PS-OC Network Bioresource Core Facility), and breast cancer associated fibroblasts (Asterand) were cultured in Dulbecco's modified Eagle's medium (DMEM) supplemented with 10% fetal bovine serum (FBS) and 100 units/ml penicillin. Human bone marrow-derived mesenchymal stem cells (MSCs) were obtained from the Tulane Center for Gene Therapy and maintained in αMEM (Invitrogen) supplemented with 20% FBS (Atlanta Biologicals) and 100 units/ml penicillin. Cells were maintained at 37 °C with 5% CO_2 in a humidified incubator and passaged every 3–4 days. Hypoxic cells (1% O_2) were maintained at 37 °C in a modular incubator chamber (Billups-Rothenberg) flushed with a gas mixture containing 1% O_2, 5% CO_2, and 94% N_2.

Real-time Reverse Transcription-Quantitative PCR—RNA extraction and cDNA synthesis were performed as published previously (33). The fold change in expression of each target mRNA relative to 18S rRNA was calculated based on the threshold cycle (C_t) as $2^{-\Delta(\Delta Ct)}$, where $\Delta C_t = C_t$ (target) $- C_t$ (18S) and $\Delta(\Delta C_t) = \Delta C_t$ (20% O_2) $- \Delta C_t$ (1% O_2).

shRNA, Lentiviruses, and Transduction—Vectors encoding shRNA targeting HIF-1α and HIF-2α were described previously (33). pLKO.1-puro expression vectors encoding shP4HA1, shP4HA2, and shPLOD2 were purchased from Sigma-Aldrich. Lentiviruses were packaged in 293T cells by co-transfection with pCMV-dR8.91 and a plasmid encoding vesicular stomatitis virus G protein using Lipofectamine 2000 (Invitrogen). Culture supernatants containing viral particles were collected 48 h after transfection and filtered (0.45-μm pore size). Fibroblasts were transduced with viral supernatant supplemented with 8 μg/ml Polybrene (Sigma-Aldrich) and selected with 0.6 μg/ml puromycin (shRNA) or zeocin (overexpression).

Immunoblot Assays—Aliquots of whole cell lysates prepared in Nonidet P-40 buffer were fractionated by 8% SDS-PAGE. Conditioned media were collected from cells and concentrated with 30% ammonium sulfate overnight at 4°C followed by centrifugation at 20,000 $\times$ *g* for 1 h. Antibodies against HIF-1α (BD Transduction Laboratory), P4HA1, P4HA2, PLOD2, HIF-2α, COL1A1 (Novus Biologicals), and β-actin (Santa Cruz Biotechnology) were used.

Atomic Force Spectroscopy Measurements—Force deformation data were acquired using a MFP one-dimensional Stand Alone atomic force microscope (Asylum Research). Analysis of data was performed using IGOR Pro, version 4.09 (WaveMetrics) integrated to the MFP analysis program (Asylum Research). MLCT-AUHW (Veeco) probes with a nominal stiffness constant of 10 piconewtons/nm were used to descend on the ECM sample by a specified distance and remain stationary for 300 ms before retracting. The forces applied during the stationary phase were binned and plotted against the distance of ECM yield. The linear slope of binned force *versus* distance of ECM yield under that force was used as the effective matrix stiffness.

Type I Collagen and Fibronectin Substrates—Cell culture plates were prepared by adding soluble rat tail type I collagen in acetic acid or fibronectin (BD Biosciences) to achieve a coverage of 33 $\mu g\ cm^{-2}$ and incubated at room temperature for 2 h. Plates were then washed gently three times with PBS and plated with cells.

Immunofluorescence and Confocal Microscopy—Cells and ECM were fixed with acetone and blocked with PBS supplemented with 10% FBS for 20 min. Fluorescent antibody against fibronectin (Alexa Fluor 568; Calbiochem) or collagen I (Alexa Fluor 488; Abcam) and DAPI (Invitrogen) were used for immunofluorescence. Fluorescent imaging was performed using confocal laser microscopy (A1; Nikon) through a 60$\times$ plan or water immersion lens (NA 1.2).

Reflection Confocal Microscopy—To visualize ECM, a Nikon A1 confocal microscope was configured to capture only reflected light from the 488-nm laser used to illuminate the sample (which was not fixed or stained) using a 60$\times$ oil-immersion objective, NA = 1.4, WD = 210 μm (Nikon).

Cell Motility Measurements—Phase contrast images were collected every 5 min using a Cascade 1K CCD camera (Roper Scientific) mounted on a Nikon TE2000E epifluorescence microscope at 10× magnification and controlled by Metamorph imaging software (Universal Imaging). Velocity was determined by tracking single cells using image recognition software (Metamorph/Metavue), with distance/time measurements taken every 5 min and then averaged for each cell. Plotting of cell displacement trajectories was performed using the x and y coordinates of each cell on each frame recorded.

Data Acquisition and Statistical Analysis—Images were analyzed and processed using MetaMorph (Molecular Devices) and NIS elements (Nikon). Morphometric analysis (length and width) was conducted in MetaMorph (Molecular Devices) for at least 50 cells/group. Fiber orientation was measured using NIS elements with built-in software for comparing orientation after thresholding. GraphPad Prism was used to calculate and plot mean ± S.E. of measured quantities, and significances were assessed by two-way analysis of variance (ANOVA).

Hydroxyproline Content Measurements—Cells were harvested and hydrolyzed in 6 N HCl for 16 h at 116 °C overnight. Tumor tissue was excised, dried in a vacuum, and weighed followed by hydrolysis in 6 N HCl for 16 h at 116 °C. Hydroxyproline content was determined by a colorimetric method (34). The total protein content was measured by the Bradford assay (Bio-Rad).

ECM Extraction—Confluent fibroblasts were incubated in 0.05% Triton-X in PBS with 10 mM NH_4OH for a maximum of 10 min. ECM was washed once with 50 mM NH_4OH in PBS followed by four or five washes in PBS and treated with DNase I (20 units/μl) for 10 min, followed by for or five additional washes in PBS.

Cell Adhesion—Cell attachment was determined by crystal violet staining. MetaMorph software (Universal Imaging) was used to calculated the optical density of cells imaged at 4×. The average value obtained on ECM of control fibroblasts at 20% O_2 was normalized to 1 as an arbitrary unit.

RESULTS

Hypoxia Regulates Fibrillar Collagen Deposition by Fibroblasts—The main fibrous proteins that constitute the ECM are collagens and fibronectin. The bulk of interstitial collagen is produced and secreted by fibroblasts that either reside in the stroma or are recruited from neighboring tissues (35). To determine the role of hypoxia on ECM fibrillogenesis, we compared fibronectin and collagen deposition by human foreskin fibroblasts cultured at 20% or 1% O_2. Immunofluorescence and confocal microscopy revealed that much of the type I collagen appeared intracellular under nonhypoxic conditions (20% O_2), whereas fibronectin was deposited extracellularly (Fig. 1*A*). Under hypoxic conditions (1% O_2), fibroblasts deposited collagen as long intact fibers that co-localized with fibronectin. To independently examine the secretion and deposition of collagen and fibronectin by fibroblasts cultured at 20% or 1% O_2, we removed the conditioned media and fibroblasts to isolate cell-free three-dimensional matrices (Fig. 1*B*). Unlike ECM derived from nonhypoxic fibroblasts, which showed punctate collagen staining, ECM produced by hypoxic fibroblasts consisted of aligned type I collagen fibers co-localized with fibronectin (Fig. 1*C*). Analysis of conditioned media revealed an increase in type I collagen secreted by hypoxic fibroblasts, without a change in secreted fibronectin levels (Fig. 1*D*). Kinetic analysis of fibroblasts cultured for 5 days under 20% or 1% O_2 revealed a dramatic induction of collagen fiber formation, which began by 3 days of exposure to 1% O_2 and increased through 5 days of continuous hypoxia, whereas fibroblasts incubated under 20% O_2 showed no change in collagen fiber formation over the 5-day time course (Fig. 1*E*). Taken together, the data presented in Fig. 1 show a dramatic and sustained increase in collagen deposition under hypoxic conditions that confirms and extends previous studies (36).

HIF-1α Is Required for Hypoxia-induced Collagen Deposition—HIF-1 has been associated with adipose, liver, and renal fibrosis (16–18). To analyze the role of HIFs in collagen production by stromal cells, we stably transfected fibroblasts with an empty vector (shEV) or vector(s) encoding shRNA against HIF-1α (sh1α), HIF-2α (sh2α), or both HIF-1α and HIF-2α (sh1/2α). Immunofluorescence of type I collagen in all fibroblast subclones cultured under 20% O_2 revealed nonfibrillar and presumably intracellular collagen localization (Fig. 2*A*). In contrast, following incubation under hypoxic conditions, type I collagen was extracellular and formed fibrillar structures in cultures of shEV fibroblasts. Fibrillar collagen deposition was blocked by knockdown of HIF-1α, or HIF-1α and HIF-2α, but not HIF-2α alone (Fig. 2*A*).

The assembly of collagen molecules into fibrils is an extracellular step in collagen biogenesis. Following secretion, procollagen molecules undergo cleavage of N- and C-terminal propeptides (which generate pC and pN, respectively). Once cleavage occurs, collagen molecules assemble spontaneously into the fibrillar structures that comprise mature collagen. We analyzed this process to determine whether hypoxia enhanced procollagen levels, secretion, or fiber formation. We separated and examined intracellular collagen, soluble extracellular collagen, and collagen incorporated into the ECM, in cultures of shEV or sh1α subclones exposed to 20% or 1% O_2. As expected, all intracellular collagen existed as a procollagen 1A1 precursor polypeptide, which migrated with an apparent molecular mass greater than 130 kDa (Fig. 2*B*, *left*). Intracellular procollagen levels decreased in response to hypoxia in shEV but not sh1α fibroblasts, suggesting that hypoxia increases procollagen secretion in a HIF-1α-dependent manner. Conditioned media from hypoxic shEV fibroblasts contained the greatest amount of fully cleaved collagen and collagen precursors (Fig. 2*B*, *middle*). ECM from cultures of hypoxic shEV cells contained more uncleaved procollagen precursor as well as cleaved and mature collagen, which were not evident in ECM from hypoxic sh1α fibroblasts or ECM from either subclone incubated at 20% O_2 (Fig. 2*B*, *right*). All forms of processed, extracellular collagen were reduced by HIF-1α knockdown. Furthermore, the increase in type I collagen deposition occurred in human MSCs and breast cancer-associated fibroblasts, two stromal cell types that are present within the tumor microenvironment (Fig. 2, *C* and *D*, and supplemental Fig. S2). Taken together, the data presented in Fig. 2 demonstrate that HIF-1 promotes procollagen secretion and cleavage, leading to the formation of mature fibrillar collagen.

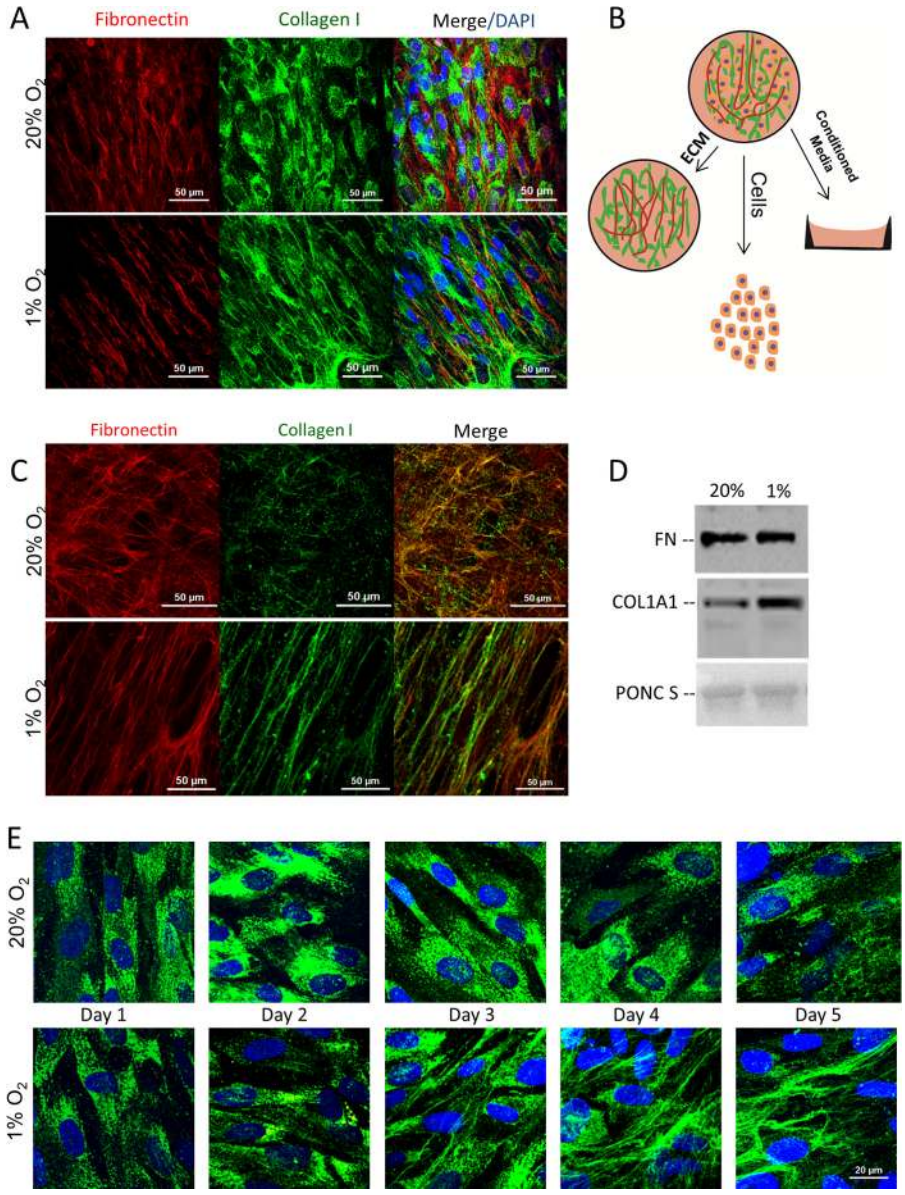

FIGURE 1. **Hypoxia regulates fibrillar collagen deposition by fibroblasts.** *A*, immunofluorescence of fibroblasts exposed to 20% or 1% O_2 for 80 h and imaged with type I collagen antibody (*green*), fibronectin antibody (*red*), and DAPI (*blue*). *B*, ECM and conditioned media were isolated from confluent fibroblast cultures following exposure to 20% or 1% O_2 for 80 h. *C*, immunofluorescence of isolated ECM for fibronectin (*red*) and type I collagen (*green*) following removal of fibroblasts (as described in *B*). *D*, immunoblot assay of fibroblast-conditioned media (as described in *B*) for type I collagen and fibronectin expression. *E*, fibroblast cultures were exposed to 20% or 1% O_2 for 1–5 days. Immunofluorescence with collagen antibody (*green*) and DAPI (*blue*) was performed at the indicated time points.

Hypoxia-induced Collagen Hydroxylase Gene Expression Is Mediated by HIF-1—Because intracellular prolyl and lysyl hydroxylation stabilizes procollagen molecules, which is necessary for secretion and fiber formation, we analyzed collagen prolyl (*P4HA1, P4HA2,* and *P4HA3*) and lysyl (*PLOD1, PLOD2,* and *PLOD3*) hydroxylase gene expression in human fibroblasts under hypoxic conditions. The expression of P4HA1, P4HA2, and PLOD2 mRNAs was induced at least 5-fold in control (shEV) cells exposed to 1% O_2 for 24 h (Fig. 3*A*). The knockdown of HIF-1α, but not HIF-2α, abrogated hypoxic induction of P4HA1, P4HA2, and PLOD2 mRNA expression (Fig. 3*A*). Immunoblot assays confirmed HIF-1α-dependent expression of P4HA1, P4HA2, and PLOD2 protein under hypoxic conditions (Fig. 3*B*). P4HA1, P4HA2, and PLOD2 protein levels were increased within 12 h of hypoxia and continued to increase over a 72-h time course (supplemental Fig. S1*A*).

To determine the effect of hypoxia-induced collagen hydroxylation on collagen biogenesis, we generated fibroblast subclones stably transfected with an empty vector (shLKO.1) or vector expressing an shRNA against PLOD2 (shPL2–1), P4HA1 (shHA1–1), or P4HA2 (shHA2–1). Immunoblot assays of the subclones confirmed the efficient knockdown of P4HA1, P4HA2, and PLOD2 in cells exposed to 20% or 1% O_2 (supplemental Fig. S1, *B* and *C*). Analysis of fibroblasts exposed to 20% or 1% O_2 for 72 h revealed that increased collagen hydroxyproline content under hypoxic conditions was blocked in HIF-1α, P4HA1, and P4HA2 knockdown cells but not in HIF-2α- or PLOD2-knockdown cells (Fig. 3*C*). Analysis of type I collagen

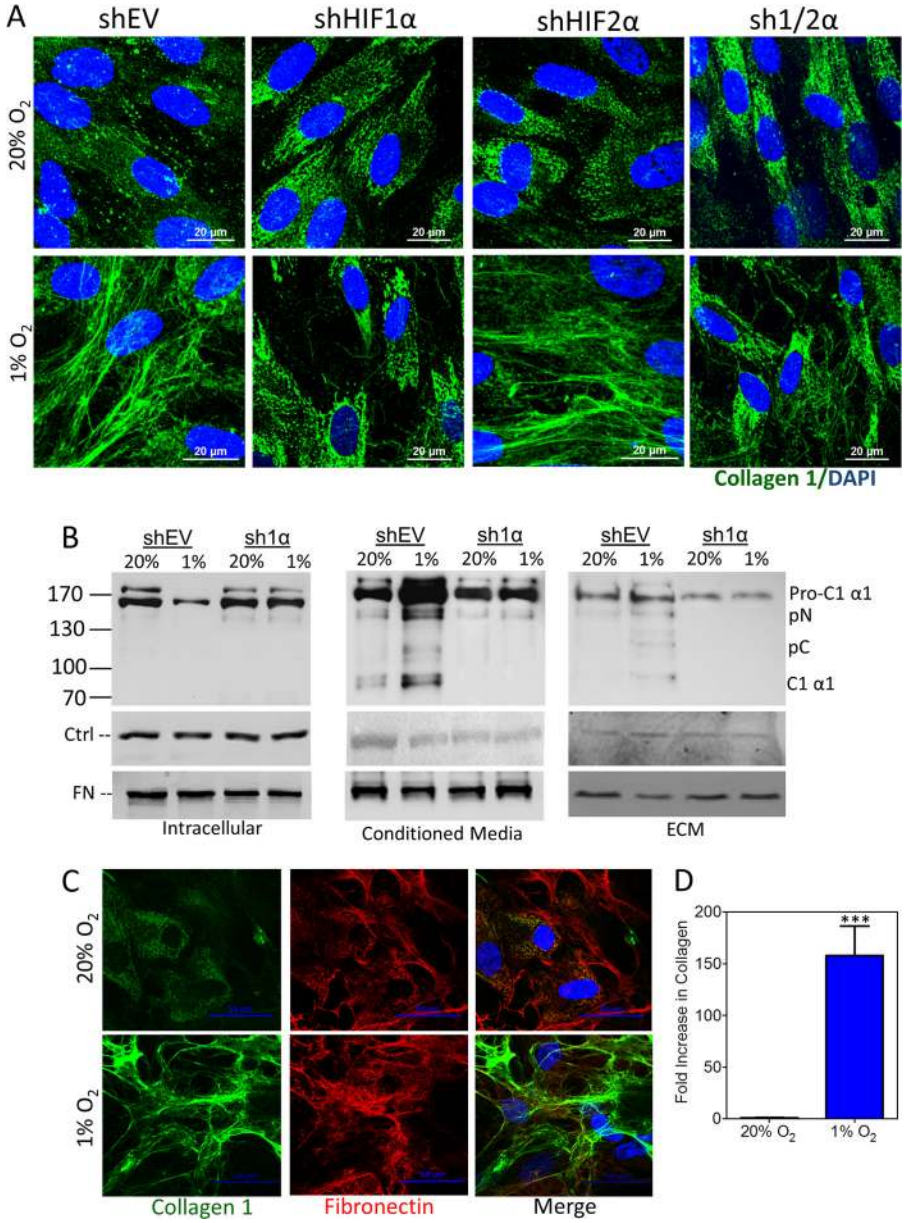

FIGURE 2. **HIF-1α promotes collagen deposition.** *A*, immunofluorescence of control (shEV), shHIF-1α (sh1α), shHIF-2α (sh2α), or shHIF-1α and shHIF-2α (sh1/2α) fibroblast subclones exposed to 20% or 1% O_2 for 80 h and imaged with type I collagen antibody (*green*) and DAPI (*blue*). *B*, immunoblot assay of cells (*left*), concentrated conditioned media (*middle*), and ECM (*right*) for type I collagen and fibronectin (*FN*). Actin levels were assessed as a loading control (*Ctrl*) in cell lysate and ECM. Ponceau S staining was used as a loading control for conditioned media. Blot indicates migration of procollagen 1α1 (*Pro-C1 α1*), N-cleaved procollagen 1α1 (*pC*), C-cleaved procollagen 1α1 (*pN*), and fully cleaved collagen (*C1 α1*). *C*, immunofluorescence of hMSCs exposed to 20% or 1% O_2 for 80 h and imaged with type I collagen antibody (*green*), fibronectin antibody (*red*), and DAPI (*blue*). *D*, intensity of immunofluorescence staining for type I collagen (*green*) quantified by image analysis and normalized to the result obtained from MSCs incubated under control (20% O_2) conditions (mean $\pm$ S.E. (*error bar*), $n = 8$); ***, $p < 0.001$ (Student's *t* test).

by immunofluorescence revealed that depletion of P4HA1 or P4HA2 inhibited hypoxia-induced fibrillar collagen deposition (Fig. 3*D*). PLOD2 knockdown resulted in a minor reduction in overall collagen deposition but a major effect on collagen fiber formation and linear organization. Analysis of an independent set of subclones expressing an shRNA targeting a different sequence in PLOD2 (shPL2-2), P4HA1 (shHA1-2), or P4HA2 (shHA2-2) showed similar results (supplemental Fig. S1, *D* and *E*).

HIF-1α-dependent Collagen Remodeling Increases ECM Alignment and Stiffness—Immunofluorescence revealed aligned collagen fibers that co-localized with fibronectin fibers after shEV fibroblasts were incubated under hypoxic conditions, whereas collagen staining of ECM derived from nonhypoxic fibroblasts was disorganized with no apparent pattern of alignment (Figs. 1, *A–C*, 2*A*, and 3*D*). To assess the impact of HIF-1 on ECM organization and compliance, we exposed shEV or sh1α fibroblasts to 20% or 1% O_2 for 72 h and extracted fibroblasts, leaving an intact cell-free ECM (Fig. 4*A*). We measured individual fibronectin fiber orientation with respect to the modal angle (set to 0°). Fibronectin fiber alignment in shEV-derived ECM was consistent with previously published results for normal fibroblasts (37). ECM derived under hypoxic conditions was more highly aligned, a characteristic that has been identified as a sign of poor prognosis in breast cancer

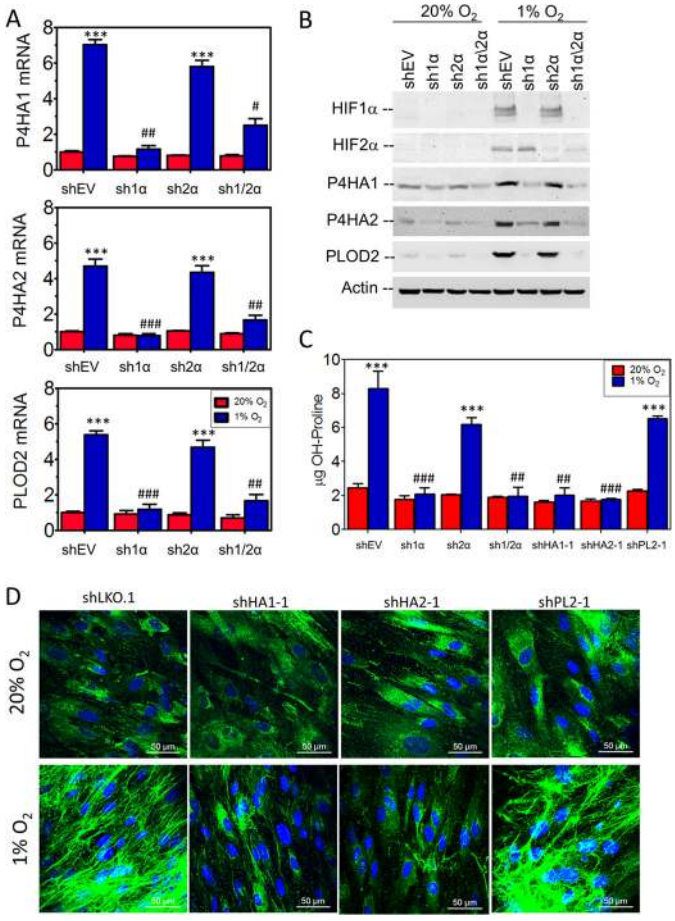

FIGURE 3. **Role of HIF-1 and collagen hydroxylases in collagen biogenesis.** *A*, collagen hydroxylase mRNA expression was analyzed by reverse transcription and quantitative real-time PCR in control (shEV), HIF-1α (sh1α), HIF-2α (sh2α), or HIF-1α and HIF-2α (sh1/2α) knockdown fibroblast subclones exposed to 20% or 1% O_2 for 24 h (mean ± S.E. (*error bars*), $n = 3$, two-way ANOVA). *B*, levels of the indicated proteins were determined by immunoblot assay following exposure of fibroblast subclones to 20% or 1% O_2 for 48 h. *C*, the hydroxyproline content of fibroblast cultures was determined following exposure to 20% or 1% O_2 for 48 h (mean ± S.E., $n = 3$, two-way ANOVA). *D*, control (shLKO.1), P4HA1 (shHA1-1), P4HA2 (shHA2-1), and PLOD2 (shPL2–1) knockdown subclones were exposed to 20% or 1% O_2 for 5 days and analyzed by immunofluorescence with type I collagen antibody (*green*) and DAPI (*blue*) followed by confocal imaging. Bonferroni post test was conducted for all two-way ANOVAs. ***, $p < 0.001$ *versus* shEV at 20% O_2; ###, $p < 0.001$; ##, $p < 0.01$; #, $p < 0.05$ *versus* shEV at 1% O_2.

tissue samples (28). The hypoxia-induced fiber alignment was abrogated by HIF-1α knockdown (Fig. 4*A*). These results identify a role for HIF-1 in defining ECM topography under hypoxic conditions.

Increased alignment of ECM fibers is characteristic of cancer compared with normal tissue (38), and the ECM in cancers is stiffer than in normal tissue (39). Moreover, highly aligned ECM is stiffer than disorganized ECM (37). Therefore, we hypothesized that ECM generated under hypoxic conditions would be stiffer than ECM generated under nonhypoxic conditions. To test this hypothesis, we measured the stiffness of cell-free ECM by atomic force spectroscopy, using a planar cantilever with contact area that was an order of magnitude greater than a single ECM fiber. The probe was held in contact with the ECM, and the distance of ECM yield was determined. The change of yield distance with change in applied force was calculated as a measure of ECM stiffness. These studies revealed that ECM derived from hypoxic fibroblasts was 3-fold stiffer than ECM derived from nonhypoxic fibroblasts (Fig. 4, *B* and *C*). Furthermore, the knockdown of HIF-1α, P4HA1, P4HA2, or PLOD2, but not HIF-2α, prevented matrix stiffening under hypoxic conditions (Fig. 4, *C* and *D*). Because PLOD2 influences matrix organization, whereas P4HA1 and P4HA2 inhibit collagen deposition, the PLOD2 knockdown data indicate that hypoxia-induced collagen fibril organization specifically enhances ECM stiffness.

HIF-1 Regulates Matrix Modulation of Cell Morphology and Adhesion—To determine how hypoxia-induced changes in ECM affect cancer cells, we isolated cell-free ECM from fibroblast subclones that were cultured in 20% or 1% O_2. Next, we plated MDA-MB-231 human breast cancer cells on the ECM preparations (Fig. 5*A*) or onto simple two-dimensional ECM substrates coated with fibronectin or type I collagen. MDA-MB-231 cells assumed a more elongated, spindle-shaped morphology on ECM from hypoxic shEV fibroblasts (Fig. 5*B*). This shape change was not observed on ECM from HIF-1α-deficient fibroblasts (Fig. 5*B* and supplemental Fig. S3*A*). To quantify this effect, we determined the elliptical factor (length/breadth of cell) for a minimum of 60 cells plated on each of the various substrates. Culturing breast cancer cells on ECM from hypoxic fibroblasts more than doubled the elliptical factor, and the effect of hypoxia was dependent on HIF-1α expression in the fibroblasts (Fig. 5*C*).

We also tested cancer cell adhesion to the fibroblast-derived ECM. Breast cancer cells preferentially aligned themselves along ECM fibers within 10 min of cell plating. Fibroblast-derived ECM was four times more effective at mediating cell adhesion than fibronectin or collagen-coated surfaces, and cell adherence was further increased by 50% on ECM derived from hypoxic fibroblasts; this effect was lost with knockdown of HIF-1α, P4HA1, or P4HA2, but not HIF-2α or PLOD2 (Fig. 5, *D–F*, and supplemental Fig. S3*B*). Taken together, these data indicate that increased HIF-1-dependent collagen deposition by hypoxic fibroblasts promotes matrix adhesion and mesenchymal morphology of breast cancer cells.

HIF-1α-dependent ECM Production Promotes Cell Migration and Directionality—Using time lapse phase contrast microscopy, we compared the motility of MDA-MB-231 cells on ECM from fibroblast subclones cultured at 20% or 1% O_2 (Fig. 6*A*). Cells plated on ECM derived from nonhypoxic fibroblasts moved randomly around their origin (supplemental Movie S1). Cells plated on ECM derived from hypoxic fibroblasts exhibited directed motion along ECM fibers (supplemental Movie S2). Cell velocity was increased by 30% on ECM generated by hypoxic fibroblasts (Fig. 6*B*). The increase in velocity elicited by ECM from hypoxic shEV fibroblasts was abrogated by the knockdown of HIF-1α but not HIF-2α. Knockdown of P4HA1, P4HA2, or PLOD2 had similar effects on cell velocity (supplemental Fig. S4*A*). Even more striking was the trajectory of cell migration on hypoxic ECM (Fig. 6*C*). The maximum distance traversed by breast cancer cells on ECM produced by hypoxic fibroblasts was 80% greater than on control ECM, and this effect was dependent on HIF-1α, P4HA1, P4HA2, and PLOD2 expression (Fig. 6*D* and supplemental Fig. S4*B*). The difference in MDA-MB-231 cell velocity and final distance traveled on

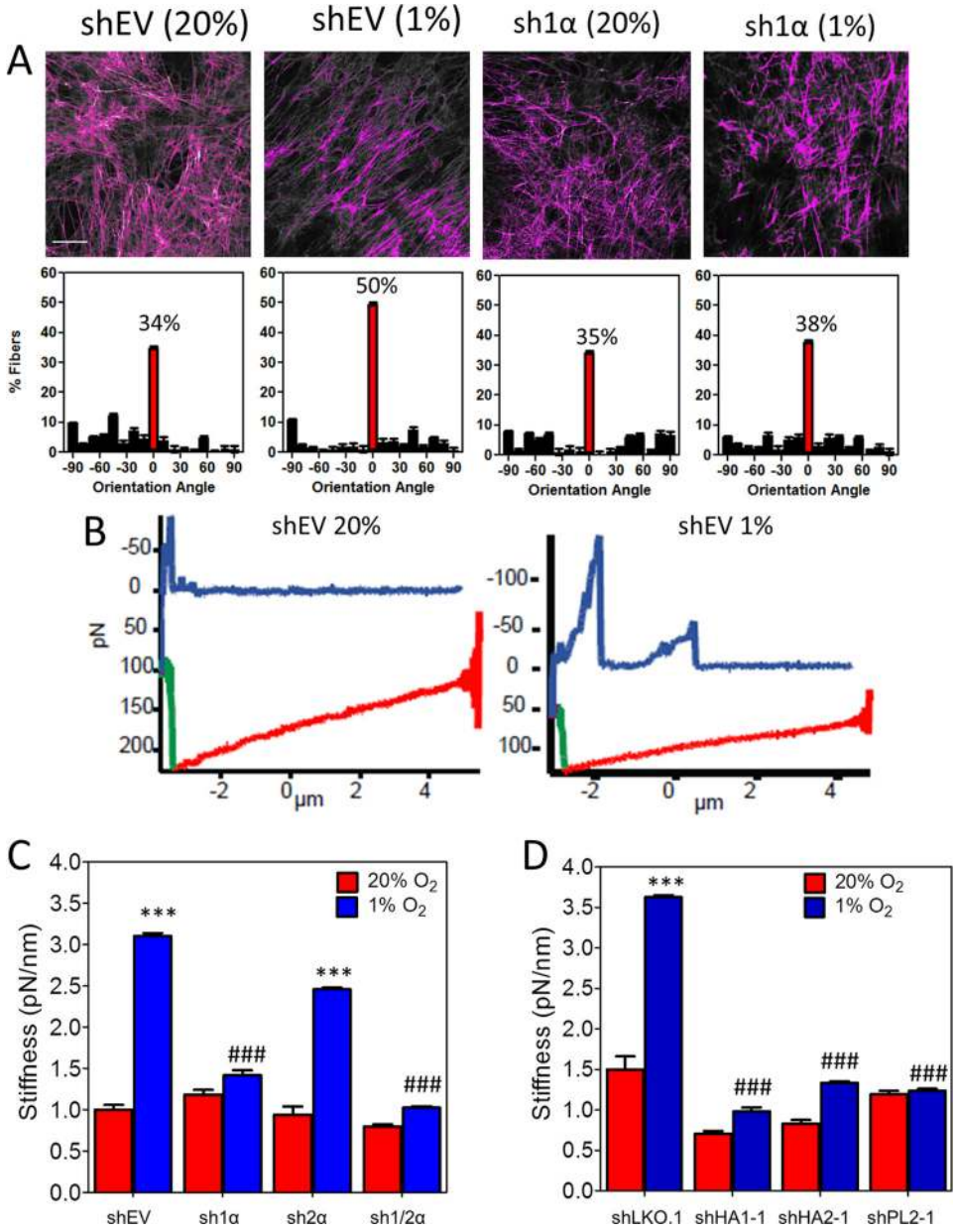

FIGURE 4. **HIF-1α promotes ECM alignment and stiffness.** *A*, fibroblast-derived ECM was generated from control (shEV) or HIF-1α–knockdown (sh1α) cells. ECM was fixed and labeled with fibronectin antibody (*upper panel*). The orientation of all thresholded fibers was quantified and plotted against the modal angle (set at 0°). Five samples/group were analyzed and plotted as a frequency distribution based on orientation angle (mean ± S.E.; lower panel). *B*, atomic force spectroscopy measurements were conducted using a probe with planar contact area applied to ECM at a constant force for 0.3 s. Force curves with descent (*red*), stationary (*green*), and ascent (*blue*) regimes for ECM derived from shEV fibroblasts exposed to 20% (*left*) or 1% (*right*) O_2 are shown. *C* and *D*, distance yielded by the ECM during the stationary regime was determined for each point probed *versus* applied force to determine the effective stiffness of ECM. Results from each impingement force were binned, and the stiffness was calculated as the slope of mean deflection over binned force (mean ± S.E. (*error bars*), $n = 30$); ***, $p < 0.001$ *versus* shEV at 20% O_2; ###, $p < 0.001$ *versus* shEV at 1% O_2 (two-way ANOVA with Bonferroni post test).

ECM that was derived from hypoxic as compared with nonhypoxic MSCs was even more dramatic (Fig. 6*F* and supplemental Fig. S4 and Movies S5 and S6).

To analyze three-dimensional interactions between breast cancer cells and the ECM, we imaged MDA-MB-231 cells migrating within fibroblast-derived ECM by time lapse reflection-confocal microscopy (Fig. 6*E* and supplemental Movies S3 and S4). To our knowledge, this is the first time that breast cancer cell migration in native ECM has been imaged using this modality. We observed that cell movement was dictated by the ECM organization, with rapid directed movement in ECM generated by hypoxic fibroblasts, whereas cells plated within control ECM were confined by the unorganized ECM. Taken together, our data demonstrate that hypoxia-induced expression of collagen prolyl and lysyl hydroxylases promotes fibrillar collagen deposition, which contributes to a more organized ECM that facilitates directional migration of breast cancer cells.

DISCUSSION

Previous studies have shown that P4HA1, P4HA2, and PLOD2 are induced under hypoxic conditions (14, 15, 32, 40). However, these studies did not investigate the consequences of

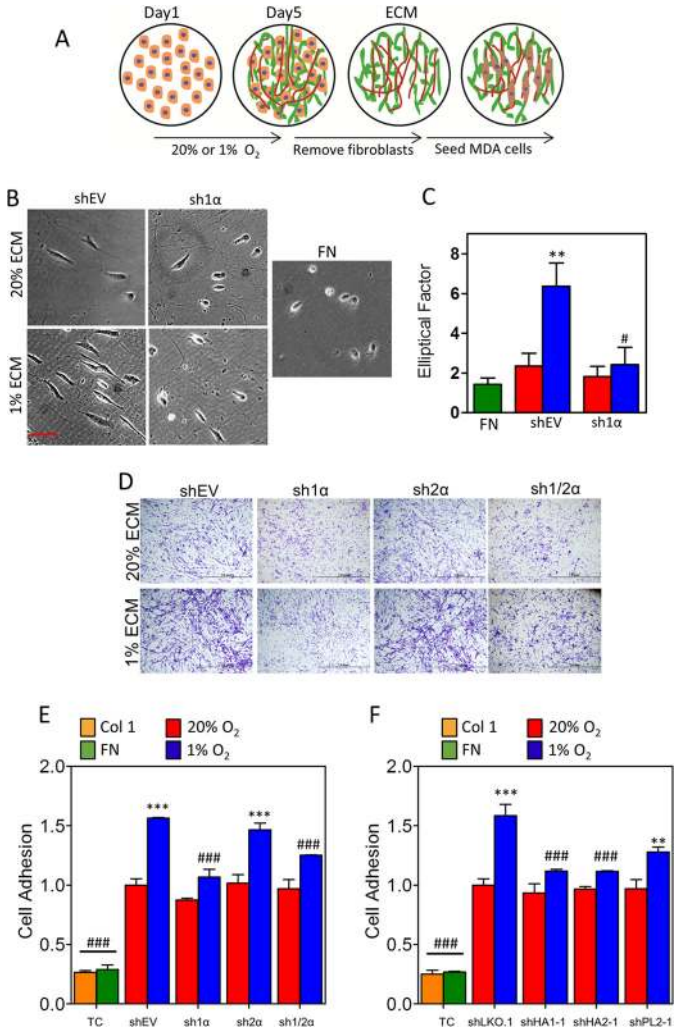

FIGURE 5. **HIF-1α regulates matrix-induced breast cancer cell morphology and adhesion.** *A*, fibroblast subclones were exposed to 20% or 1% O_2 for 5 days. Fibroblast-derived ECM was isolated, and naive MDA-MB-231 cells were plated at low confluence within the ECM. *B*, phase contrast image of MDA-MB-231 cells, which were either plated on ECM derived from shEV or sh1α fibroblasts that were incubated under 20% or 1% O_2 (*left*) or plated on fibronectin (*FN*; *right*) is shown. *Scale bar*, 100 μm (same scale for all micrographs). *C*, the elliptical factor (length/breadth ratio) was calculated for MDA-MB-231 cells plated on fibronectin or on ECM derived from shEV or sh1α fibroblasts incubated under 20% or 1% O_2 (mean $\pm$ S.E. (*error bars*), $n > 60$, two-way ANOVA with Bonferroni post test); **, $p < 0.01$ *versus* shEV at 20% O_2; #, $p < 0.05$ *versus* shEV at 1% O_2. *D*, MDA-MB-231 cells were plated on ECM from the indicated fibroblast subclones that were exposed to 20% or 1% O_2 for 80 h. MDA-MB-231 cells were allowed to adhere to ECM for 20 min, non-adherent cells were washed off, and adherent cells were stained with crystal violet. *E* and *F*, MDA-MB-231 cells were plated on collagen or fibronectin-coated plates or on ECM from the indicated subclones that were exposed to 20% or 1% O_2 for 80 h. Adhesion was quantified by optical density measurements of stained cells (mean $\pm$ S.E., $n = 5$, two-way ANOVA with Bonferroni post test). **, $p < 0.01$; ***, $p < 0.001$ *versus* control (shEV or shLKO.1) at 20% O_2; ###, $p < 0.001$ *versus* control at 1% O_2.

changes in hydroxylase expression on collagen deposition or changes in the physical properties of the matrix, such as stiffness. In addition, the role of HIF-1-induced collagen deposition on cell-ECM interactions, such as adhesion, motility, or spreading, has never been reported. In this study, we report that HIF-1-regulated expression of collagen prolyl and lysyl hydroxylases affects the composition and mechanical properties of human fibroblast-derived ECM. We demonstrate that HIF-1α-dependent expression of collagen prolyl and lysyl hydroxylases is required for proper collagen fiber formation in response to hypoxia. Analysis of breast cancer-associated fibroblasts revealed even greater effects of hypoxia on collagen deposition. Our results show that HIF-1 activation in human fibroblasts regulates ECM biogenesis to produce a stiff microenvironment that enhances cell adhesion, elongation, and motility. HIF-1 mediates these events by increasing procollagen prolyl (P4HA1 and P4HA2) and lysyl (PLOD2) hydroxylase expression in hypoxic fibroblasts, resulting in increased fibrillar collagen deposition. Our data suggest that HIF-1-dependent collagen modification is critical for dynamic matrix organization and stiffness, which are defining characteristics of cancer and other diseases that are associated with tissue fibrosis.

HIF-1 Regulates Collagen Biogenesis—Multiple sequential steps are required for collagen fiber formation, including translation of procollagen polypeptides, hydroxylation of prolyl and lysyl residues, triple helix formation, glycosylation, secretion to the extracellular space, cleavage of propeptides, fiber formation, and cross-linking of collagen fibers. Several studies have highlighted the role of HIF-1 in stimulating fibrosis in renal (18) and adipose (16) tissue as well as ECM cross-linking in cancer (41–43) through the activation of lysyl oxidase family members, which are enzymes that cross-link collagen fibers after extracellular deposition. Using fibroblast-derived ECM, our study investigated the stepwise regulation of collagen biogenesis (Figs. 1–3). With this approach, we demonstrated the importance of HIF-1 in regulating extracellular collagen accumulation in conditioned media as well as collagen fiber formation in ECM to form a fibrotic microenvironment (Fig. 2*B*). We showed that HIF-1 promotes intracellular processing of collagen (Fig. 3), which enhances collagen deposition and subsequent cross-linking by lysyl oxidases. These findings, taken together with the dramatic effect of P4HA1, P4HA2, and PLOD2 knockdown on collagen deposition and/or fiber formation demonstrate the requirement for HIF-1α in collagen fiber formation prior to collagen cross-linking by lysyl oxidases. Taken together with previous studies (16, 17, 39, 43), these new findings show that HIF-1 coordinately regulates multiple intracellular and extracellular steps in collagen biogenesis.

Deposition of collagen and ECM accompanies tumor progression. Although the desmoplastic response to tumor formation that is enhanced by recruitment of cancer-associated fibroblasts and macrophages has been reported (44, 45), the underlying molecular mechanisms have remained relatively undefined. Our results suggest that intratumoral hypoxia, which is a common finding in the majority of solid cancers, leads to tumor fibrosis by HIF-1-mediated induction of procollagen prolyl and lysyl hydroxylase expression by stromal fibroblasts. Ongoing studies suggest that cancer cells also contribute to ECM remodeling in response to hypoxia (54).

HIF-1α-dependent ECM Alignment Alters Cancer Cell Morphology and Directional Motility—Through reciprocal cell-ECM interactions, the stroma provides cues that are essential for tissue architecture. The fibroblast-derived ECM in our study models the physiological microenvironment of cell-matrix interactions. Cell-free three-dimensional matrices generated by hypoxic shEV fibroblasts contained fibers that were

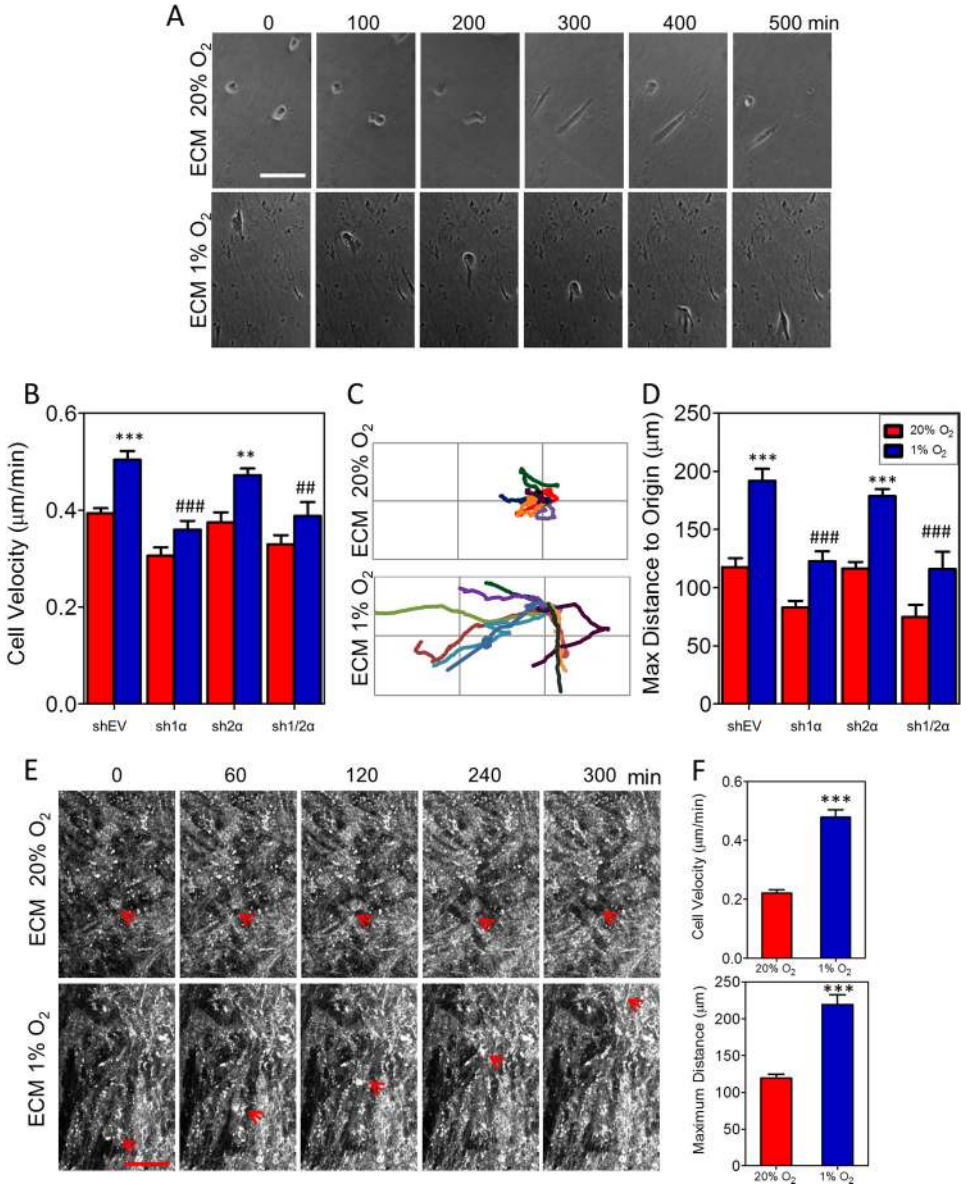

FIGURE 6. **HIF-1α-dependent ECM production stimulates cancer cell migration and directionality.** *A*, phase contrast microscopy images of MDA-MB-231 cells migrating for 300 min on ECM from fibroblasts exposed to 20% or 1% O_2 for 72 h. *Scale bar*, 120 μm. *B*, velocity of MDA-MB-231 cells migrating on ECM from the indicated fibroblast subclones, which were exposed to 20% or 1% O_2 for 80 h (mean $\pm$ S.E. (*error bars*), $n = 90$, two-way ANOVA). *C*, representative trajectories of individual MDA-MB-231 cells (marked with different *colors*) migrating on fibroblast-derived ECM were tracked for 14 h using phase contrast microscopy. Gridlines are 100 μm (height) by 200 μm (width). *D*, the straight-line distance from the cell at its origin to its final position determined using the initial (0, 0) and final (x, y) position coordinates (mean $\pm$ S.E., $n = 90$, two-way ANOVA). *E*, reflection confocal microscopy images of MDA-MB-231 cells migrating over time within fibroblast-derived ECM. Location of the migrating cell is indicated by the *red arrow*. *Scale bar*, 70 μm. Bonferroni post test was conducted for all ANOVA experiments; ***, $p < 0.001$; **, $p < 0.01$ *versus* ECM from shEV at 20% O_2; ###, $p < 0.001$; ##, $p < 0.01$ *versus* ECM from shEV at 1% O_2. *F*, velocity (*upper panel*) and distance from the cell at its origin to its final position (*lower panel*) of MDA-MB-231 cells migrating on ECM from MSCs exposed to 20% or 1% O_2 for 80 h (mean $\pm$ S.E., $n = 40$, Student's t test); ***, $p < 0.001$.

more aligned than matrices derived from hypoxic HIF-1α-, PLOD2-, P4HA1-, or P4HA2-deficient fibroblasts (Fig. 4). Thus, hypoxic fibroblasts remodel ECM in a HIF-1-dependent manner to provide contact guidance to surrounding cells within a tissue. The morphology of the breast cancer cells tested was strongly influenced by the architecture of the matrix. Recent studies have shown that contact guidance occurs within tumors, in which fiber alignment in the ECM guides local invasion and predicts patient mortality in breast cancers (28, 29, 46). *In vivo* analysis of cancer cell migration revealed that collagen fiber alignment is crucial to directing cell motility (30). Cells preferentially invade along aligned collagen fibers compared with randomly organized collagen (47). Indeed, the migration of MDA-MB-231 cells was directionally persistent on ECM from hypoxic shEV fibroblasts (Fig. 6). These data suggest that hypoxic stromal cells within breast cancers may promote invasion and metastasis through HIF-1-dependent ECM remodeling.

Fibrillar collagen also affects biophysical signaling between cells and their microenvironment. Matrix stiffness disrupts tissue morphogenesis (48) and drives the differentiation of MSCs (49). In studies of tumor progression and metastasis, collagen

cross-linking by lysyl oxidase increased tissue stiffness and resulted in enhanced ECM-cell interactions that were important for cell invasion (39). However, studies using tumor tissue do not directly measure the contribution of the ECM alone to the tumor tissue. In our study, we utilized ECM derived from fibroblasts to show that HIF-1α or procollagen hydroxylase knockdown specifically reduced the stiffness of hypoxic ECM (Fig. 4). These data indicate that both ECM stiffness and fiber alignment under hypoxic conditions can increase the invasiveness of breast cancer cells. These findings are consistent with increasing evidence indicating that HIF-1 plays multiple critical roles in breast cancer metastasis (33, 43, 50–54).

Differential Effect of Prolyl versus Lysyl Hydroxylation on Cell-Matrix Interactions—In our study, prolyl hydroxylation was required for collagen deposition, whereas lysyl hydroxylation promoted overall fiber formation under hypoxic conditions (Fig. 3*D*). The knockdown of P4HA1, P4HA2, or PLOD2 reduced matrix stiffness and matrix-induced cell morphology and directed cell migration (Fig. 4, *B* and *D*, and supplemental Fig. S4). However, only knockdown of P4HA1 or P4HA2 abrogated cell adhesion (Fig. 5*F*). This result suggests that increased collagen deposition under hypoxic conditions is sufficient for enhanced cell-matrix adhesion, whereas collagen fiber formation is strictly required to enhance directed cancer cell migration.

A growing body of evidence indicates that ECM remodeling is essential for normal tissue architecture and is altered in many disease states. Our study identifies a critical role of hypoxia and HIF-1 in the regulation of matrix-dependent cell behavior. Further elucidation of the consequences of this regulation in the context of disease may lead to novel treatment strategies for cancer and other disorders associated with increased tissue fibrosis.

Acknowledgment—We thank Karen Padgett of Novus Biologicals for generous gifts of antibodies against HIF-2α, P4HA1, P4HA2, PLOD2, and COL1A1.

REFERENCES

1. Frantz, C., Stewart, K. M., and Weaver, V. M. (2010) The extracellular matrix at a glance. *J. Cell Sci.* **123,** 4195–4200
2. Hynes, R. O. (2009) The extracellular matrix: not just pretty fibrils. *Science* **326,** 1216–1219
3. Järveläinen, H., Sainio, A., Koulu, M., Wight, T. N., and Penttinen, R. (2009) Extracellular matrix molecules: potential targets in pharmacotherapy. *Pharmacol. Rev.* **61,** 198–223
4. Myllyharju, J., and Kivirikko, K. I. (2004) Collagens, modifying enzymes and their mutations in humans, flies and worms. *Trends Genet.* **20,** 33–43
5. Myllyharju, J. (2003) Prolyl 4-hydroxylases, the key enzymes of collagen biosynthesis. *Matrix Biol.* **22,** 15–24
6. Annunen, P., Helaakoski, T., Myllyharju, J., Veijola, J., Pihlajaniemi, T., and Kivirikko, K. I. (1997) Cloning of the human prolyl 4-hydroxylase α subunit isoform α(II) and characterization of the type II enzyme tetramer. The α(I) and α(II) subunits do not form a mixed α(I)α(II)β2 tetramer. *J. Biol. Chem.* **272,** 17342–17348
7. Kukkola, L., Hieta, R., Kivirikko, K. I., and Myllyharju, J. (2003) Identification and characterization of a third human, rat, and mouse collagen prolyl 4-hydroxylase isoenzyme. *J. Biol. Chem.* **278,** 47685–47693
8. Valtavaara, M., Szpirer, C., Szpirer, J., and Myllylä, R. (1998) Primary structure, tissue distribution, and chromosomal localization of a novel isoform of lysyl hydroxylase (lysyl hydroxylase 3). *J. Biol. Chem.* **273,** 12881–12886
9. Steinmann, B., and Raghunath, M. (1995) Delayed helix formation of mutant collagen. *Science* **267,** 258
10. Yeowell, H. N., Walker, L. C., Murad, S., and Pinnell, S. R. (1997) A common duplication in the lysyl hydroxylase gene of patients with Ehlers-Danlos syndrome type VI results in preferential stimulation of lysyl hydroxylase activity and mRNA by hydralazine. *Arch. Biochem. Biophys.* **347,** 126–131
11. Steinmann, B., Eyre, D. R., and Shao, P. (1995) Urinary pyrridinoline cross-links in Ehlers-Danlos syndrome type VI. *Am. J. Hum. Genet.* **57,** 1505–1508
12. van der Slot, A. J., Zuurmond, A. M., Bardoel, A. F., Wijmenga, C., Pruijs, H. E., Sillence, D. O., Brinckmann, J., Abraham, D. J., Black, C. M., Verzijl, N., DeGroot, J., Hanemaaijer, R., TeKoppele, J. M., Huizinga, T. W., and Bank, R. A. (2003) Identification of PLOD2 as telopeptide lysyl hydroxylase, an important enzyme in fibrosis. *J. Biol. Chem.* **278,** 40967–40972
13. Brinckmann, J., Açil, Y., Tronnier, M., Notbohm, H., Bätge, B., Schmeller, W., Koch, M. H., Müller, P. K., and Wolff, H. H. (1996) Altered x-ray diffraction pattern is accompanied by a change in the mode of cross-link formation in lipodermatosclerosis. *J. Invest. Dermatol.* **107,** 589–592
14. Myllyharju, J., and Schipani, E. (2010) Extracellular matrix genes as hypoxia-inducible targets. *Cell Tissue Res.* **339,** 19–29
15. Hofbauer, K. H., Gess, B., Lohaus, C., Meyer, H. E., Katschinski, D., and Kurtz, A. (2003) Oxygen tension regulates the expression of a group of procollagen hydroxylases. *Eur. J. Biochem.* **270,** 4515–4522
16. Halberg, N., Khan, T., Trujillo, M. E., Wernstedt-Asterholm, I., Attie, A. D., Sherwani, S., Wang, Z. V., Landskroner-Eiger, S., Dineen, S., Magalang, U. J., Brekken, R. A., and Scherer, P. E. (2009) Hypoxia-inducible factor 1α induces fibrosis and insulin resistance in white adipose tissue. *Mol. Cell. Biol.* **29,** 4467–4483
17. Moon, J. O., Welch, T. P., Gonzalez, F. J., and Copple, B. L. (2009) Reduced liver fibrosis in hypoxia-inducible factor-1α-deficient mice. *Am. J. Physiol. Gastrointest. Liver Physiol.* **296,** G582–592
18. Higgins, D. F., Kimura, K., Bernhardt, W. M., Shrimanker, N., Akai, Y., Hohenstein, B., Saito, Y., Johnson, R. S., Kretzler, M., Cohen, C. D., Eckardt, K. U., Iwano, M., and Haase, V. H. (2007) Hypoxia promotes fibrogenesis *in vivo* via HIF-1 stimulation of epithelial-to-mesenchymal transition. *J. Clin. Invest.* **117,** 3810–3820
19. Gillies, R. J., and Gatenby, R. A. (2007) Hypoxia and adaptive landscapes in the evolution of carcinogenesis. *Cancer Metastasis Rev.* **26,** 311–317
20. Wang, G. L., Jiang, B. H., Rue, E. A., and Semenza, G. L. (1995) Hypoxia-inducible factor 1 is a basic-helix-loop-helix-PAS heterodimer regulated by cellular O_2 tension. *Proc. Natl. Acad. Sci. U.S.A.* **92,** 5510–5514
21. Semenza, G. L. (2010) Defining the role of hypoxia-inducible factor 1 in cancer biology and therapeutics. *Oncogene* **29,** 625–634
22. Semenza, G. L. (2009) Regulation of oxygen homeostasis by hypoxia-inducible factor 1. *Physiology* **24,** 97–106
23. Bos, R., van der Groep, P., Greijer, A. E., Shvarts, A., Meijer, S., Pinedo, H. M., Semenza, G. L., van Diest, P. J., and van der Wall, E. (2003) Levels of hypoxia-inducible factor-1α independently predict prognosis in patients with lymph node negative breast carcinoma. *Cancer* **97,** 1573–1581
24. Schindl, M., Schoppmann, S. F., Samonigg, H., Hausmaninger, H., Kwasny, W., Gnant, M., Jakesz, R., Kubista, E., Birner, P., and Oberhuber, G. (2002) Overexpression of hypoxia-inducible factor 1α is associated with an unfavorable prognosis in lymph node-positive breast cancer. *Clin. Cancer Res.* **8,** 1831–1837
25. Generali, D., Berruti, A., Brizzi, M. P., Campo, L., Bonardi, S., Wigfield, S., Bersiga, A., Allevi, G., Milani, M., Aguggini, S., Gandolfi, V., Dogliotti, L., Bottini, A., Harris, A. L., and Fox, S. B. (2006) Hypoxia-inducible factor-1α expression predicts a poor response to primary chemoendocrine therapy and disease-free survival in primary human breast cancer. *Clin. Cancer Res.* **12,** 4562–4568
26. Yamamoto, Y., Ibusuki, M., Okumura, Y., Kawasoe, T., Kai, K., Iyama, K., and Iwase, H. (2008) Hypoxia-inducible factor 1α is closely linked to an aggressive phenotype in breast cancer. *Breast Cancer Res. Treat.* **110,** 465–475
27. Dales, J. P., Garcia, S., Meunier-Carpentier, S., Andrac-Meyer, L., Haddad,

O., Lavaut, M. N., Allasia, C., Bonnier, P., and Charpin, C. (2005) Overexpression of hypoxia-inducible factor HIF-1α predicts early relapse in breast cancer: retrospective study in a series of 745 patients. *Int. J. Cancer* **116,** 734–739

28. Conklin, M. W., Eickhoff, J. C., Riching, K. M., Pehlke, C. A., Eliceiri, K. W., Provenzano, P. P., Friedl, A., and Keely, P. J. (2011) Aligned collagen is a prognostic signature for survival in human breast carcinoma. *Am. J. Pathol.* **178,** 1221–1232
29. Provenzano, P. P., Eliceiri, K. W., Campbell, J. M., Inman, D. R., White, J. G., and Keely, P. J. (2006) Collagen reorganization at the tumor-stromal interface facilitates local invasion. *BMC Med.* **4,** 38
30. Wyckoff, J. B., Wang, Y., Lin, E. Y., Li, J. F., Goswami, S., Stanley, E. R., Segall, J. E., Pollard, J. W., and Condeelis, J. (2007) Direct visualization of macrophage-assisted tumor cell intravasation in mammary tumors. *Cancer Res.* **67,** 2649–2656
31. Wang, W., Wyckoff, J. B., Frohlich, V. C., Oleynikov, Y., Hüttelmaier, S., Zavadil, J., Cermak, L., Bottinger, E. P., Singer, R. H., White, J. G., Segall, J. E., and Condeelis, J. S. (2002) Single cell behavior in metastatic primary mammary tumors correlated with gene expression patterns revealed by molecular profiling. *Cancer Res.* **62,** 6278–6288
32. Aro, E., Khatri, R., Gerard-O'Riley, R., Mangiavini, L., Myllyharju, J., and Schipani, E. (2012) Hypoxia-inducible factor-1 (HIF-1) but not HIF-2 is essential for hypoxic induction of collagen prolyl 4-hydroxylases in primary newborn mouse epiphyseal growth plate chondrocytes. *J. Biol. Chem.* **287,** 37134–37144
33. Zhang, H., Wong, C. C., Wei, H., Gilkes, D. M., Korangath, P., Chaturvedi, P., Schito, L., Chen, J., Krishnamachary, B., Winnard, P. T., Jr., Raman, V., Zhen, L., Mitzner, W. A., Sukumar, S., and Semenza, G. L. (2012) HIF-1-dependent expression of angiopoietin-like 4 and L1CAM mediates vascular metastasis of hypoxic breast cancer cells to the lungs. *Oncogene* **31,** 1757–1770
34. Reddy, G. K., and Enwemeka, C. S. (1996) A simplified method for the analysis of hydroxyproline in biological tissues. *Clin. Biochem.* **29,** 225–229
35. De Wever, O., Demetter, P., Mareel, M., and Bracke, M. (2008) Stromal myofibroblasts are drivers of invasive cancer growth. *Int. J. Cancer* **123,** 2229–2238
36. Horino, Y., Takahashi, S., Miura, T., and Takahashi, Y. (2002) Prolonged hypoxia accelerates the posttranscriptional process of collagen synthesis in cultured fibroblasts. *Life Sci.* **71,** 3031–3045
37. Goetz, J. G., Minguet, S., Navarro-Lérida, I., Lazcano, J. J., Samaniego, R., Calvo, E., Tello, M., Osteso-Ibáñez, T., Pellinen, T., Echarri, A., Cerezo, A., Klein-Szanto, A. J., Garcia, R., Keely, P. J., Sánchez-Mateos, P., Cukierman, E., and Del Pozo, M. A. (2011) Biomechanical remodeling of the microenvironment by stromal caveolin-1 favors tumor invasion and metastasis. *Cell* **146,** 148–163
38. Provenzano, P. P., Eliceiri, K. W., and Keely, P. J. (2009) Multiphoton microscopy and fluorescence lifetime imaging microscopy (FLIM) to monitor metastasis and the tumor microenvironment. *Clin. Exp. Metastasis* **26,** 357–370
39. Levental, K. R., Yu, H., Kass, L., Lakins, J. N., Egeblad, M., Erler, J. T., Fong, S. F., Csiszar, K., Giaccia, A., Weninger, W., Yamauchi, M., Gasser, D. L., and Weaver, V. M. (2009) Matrix crosslinking forces tumor progression by enhancing integrin signaling. *Cell* **139,** 891–906
40. Takahashi, Y., Takahashi, S., Shiga, Y., Yoshimi, T., and Miura, T. (2000) Hypoxic induction of prolyl 4-hydroxylase α (I) in cultured cells. *J. Biol. Chem.* **275,** 14139–14146
41. Erler, J. T., Bennewith, K. L., Nicolau, M., Dornhöfer, N., Kong, C., Le, Q. T., Chi, J. T., Jeffrey, S. S., and Giaccia, A. J. (2006) Lysyl oxidase is essential for hypoxia-induced metastasis. *Nature* **440,** 1222–1226
42. Erler, J. T., Bennewith, K. L., Cox, T. R., Lang, G., Bird, D., Koong, A., Le, Q. T., and Giaccia, A. J. (2009) Hypoxia-induced lysyl oxidase is a critical mediator of bone marrow cell recruitment to form the premetastatic niche. *Cancer Cell* **15,** 35–44
43. Wong, C. C., Gilkes, D. M., Zhang, H., Chen, J., Wei, H., Chaturvedi, P., Fraley, S. I., Wong, C. M., Khoo, U. S., Ng, I. O., Wirtz, D., and Semenza, G. L. (2011) Hypoxia-inducible factor 1 is a master regulator of breast cancer metastatic niche formation. *Proc. Natl. Acad. Sci. U.S.A.* **108,** 16369–16374
44. Ingman, W. V., Wyckoff, J., Gouon-Evans, V., Condeelis, J., and Pollard, J. W. (2006) Macrophages promote collagen fibrillogenesis around terminal end buds of the developing mammary gland. *Dev. Dyn.* **235,** 3222–3229
45. Leek, R. D., and Harris, A. L. (2002) Tumor-associated macrophages in breast cancer. *J. Mammary Gland Biol. Neoplasia* **7,** 177–189
46. Provenzano, P. P., Eliceiri, K. W., Inman, D. R., and Keely, P. J. (2010) *Curr. Protoc. Cell Biol.* **Chapter 10,** Unit 10.17
47. Provenzano, P. P., Inman, D. R., Eliceiri, K. W., Trier, S. M., and Keely, P. J. (2008) Contact guidance mediated three-dimensional cell migration is regulated by Rho/ROCK-dependent matrix reorganization. *Biophys. J.* **95,** 5374–5384
48. Paszek, M. J., Zahir, N., Johnson, K. R., Lakins, J. N., Rozenberg, G. I., Gefen, A., Reinhart-King, C. A., Margulies, S. S., Dembo, M., Boettiger, D., Hammer, D. A., and Weaver, V. M. (2005) Tensional homeostasis and the malignant phenotype. *Cancer Cell* **8,** 241–254
49. Engler, A. J., Sen, S., Sweeney, H. L., and Discher, D. E. (2006) Matrix elasticity directs stem cell lineage specification. *Cell* **126,** 677–689
50. Schito, L., Rey, S., Tafani, M., Zhang, H., Wong, C. C., Russo, A., Russo, M. A., and Semenza, G. L. (2012) Hypoxia-inducible factor 1-dependent expression of platelet-derived growth factor B promotes lymphatic metastasis of hypoxic breast cancer cells. *Proc. Natl. Acad. Sci. U.S.A.* **109,** E2707–2716
51. Wong, C. C., Zhang, H., Gilkes, D. M., Chen, J., Wei, H., Chaturvedi, P., Hubbi, M. E., and Semenza, G. L. (2012) Inhibitors of hypoxia-inducible factor 1 block breast cancer metastatic niche formation and lung metastasis. *J. Mol. Med.* **90,** 803–815
52. Luo, W., Chang, R., Zhong, J., Pandey, A., and Semenza, G. L. (2012) Histone demethylase JMJD2C is a coactivator for hypoxia-inducible factor 1 that is required for breast cancer progression. *Proc. Natl. Acad. Sci. U.S.A.* **109,** E3367–3376
53. Chaturvedi, P., Gilkes, D. M., Wong, C. C., Kshitiz, Luo, W., Zhang, H., Wei, H., Takano, N., Schito, L., Levchenko, A., and Semenza, G. L. (2013) Hypoxia-inducible factor-dependent breast cancer-mesenchymal stem cell bidirectional signaling promotes metastasis. *J. Clin. Invest.* **123,** 189–205
54. Gilkes, D. M., Bajpai, S., Wong, C. C., Chaturvedi, P., Hubbi, M. E., Wirtz, D., and Semenza, G. L. (2013) Procollagen lysyl hydroxylase 2 is essential for breast cancer metastasis. *Mol. Cancer Res.* DOI: 10.1158/1541–7786.MCR-12–0629